High-resolution Mapping of Urban Land Use Intensity in Watersheds of the St. Louis River Estuary

George Host, Paul Meysembourg and Lucinda Johnson
Natural Resources Research Institute
University of Minnesota Duluth
Duluth, MN

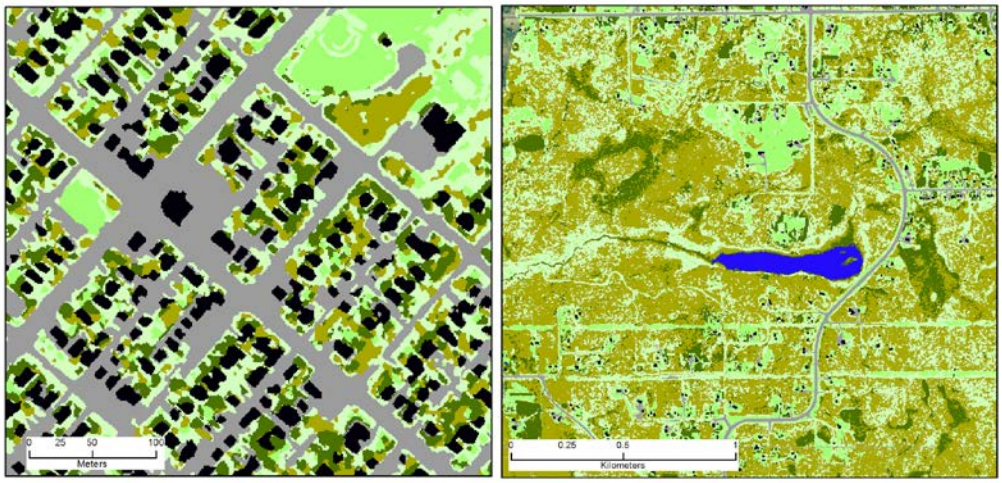

Final Report to
National Oceanic and Atmospheric Administration
Office of Coastal Management

Administered by

Woolpert
116 Inverness Drive East, Suite 105
Englewood, CO 80112

July 2015
NRRI/TR-2015/41

Introduction

Agriculture and development are the source of a multitude of environmental stressors influencing coastal ecosystems, including sediment and nutrient runoff, alterations to hydrologic and thermal regimes, delivery of pollutants and loss of habitat. Many studies have addressed the effects of land use on aquatic ecosystem (see Johnson and Host 2010 for a detailed literature review), but fundamental issues of scale remain unresolved. In a recent study, Stueve et al. (2014) demonstrate the dramatic differences in resolution and subsequent estimates of watershed-scale land use between the commonly-used National Land Cover Dataset (NLCD) and a high resolution classification based on aerial photography, LiDAR and other imagery (Figure 1).

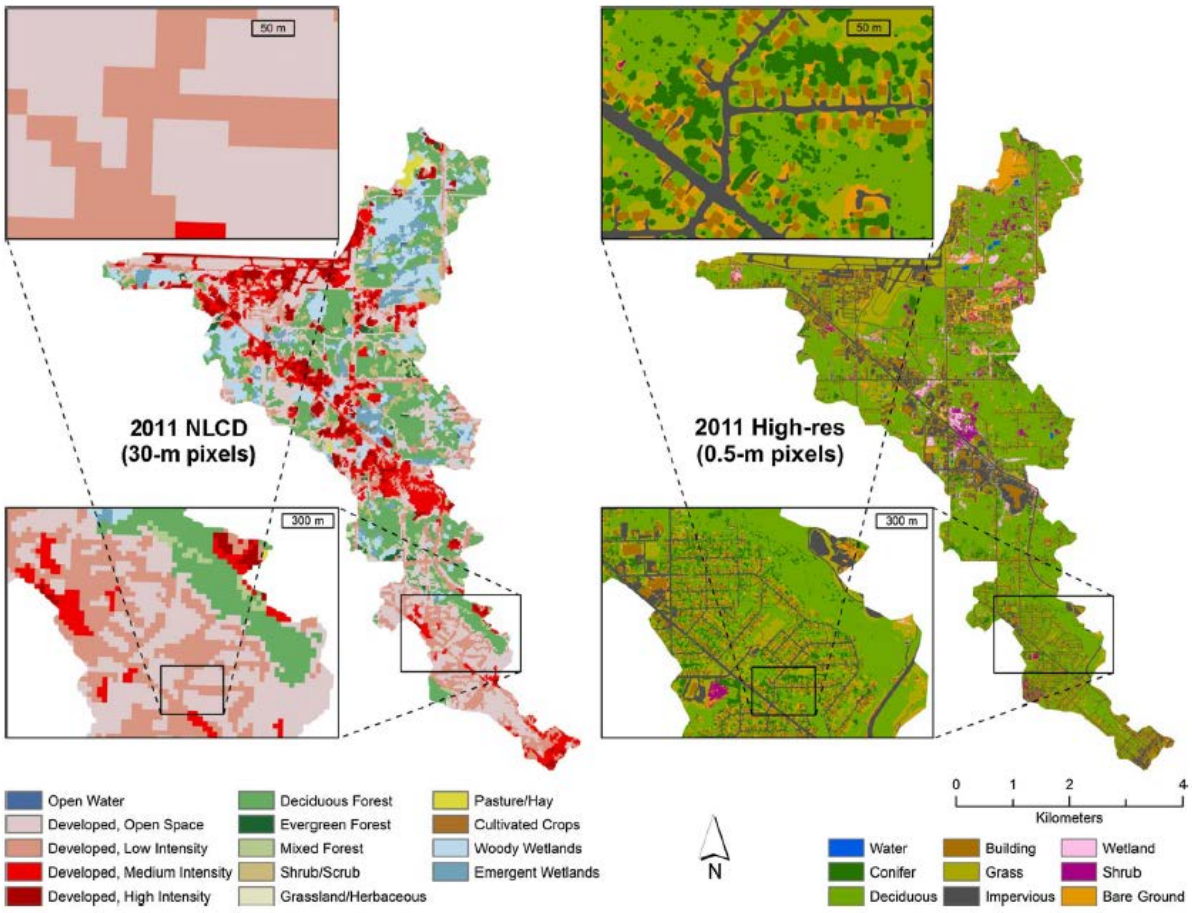

Figure 1 Comparison of NLCD and high resolution classification in identical areas in Miller Creek watershed, Duluth, MN

Land use data are common inputs to environmental indicator development, hydrologic models such as SWMM or HSPF, and decision support models such as the EPA National Stormwater Calculator. The difference in areal estimates of urban land cover between NLCD and higher resolution land classification can result in significant differences in predicted amounts of runoff

and infiltration (Figure 2). Using these data to develop remediation strategies using green or gray infrastructure could potentially result in costly errors through under or over-engineering retention structures.

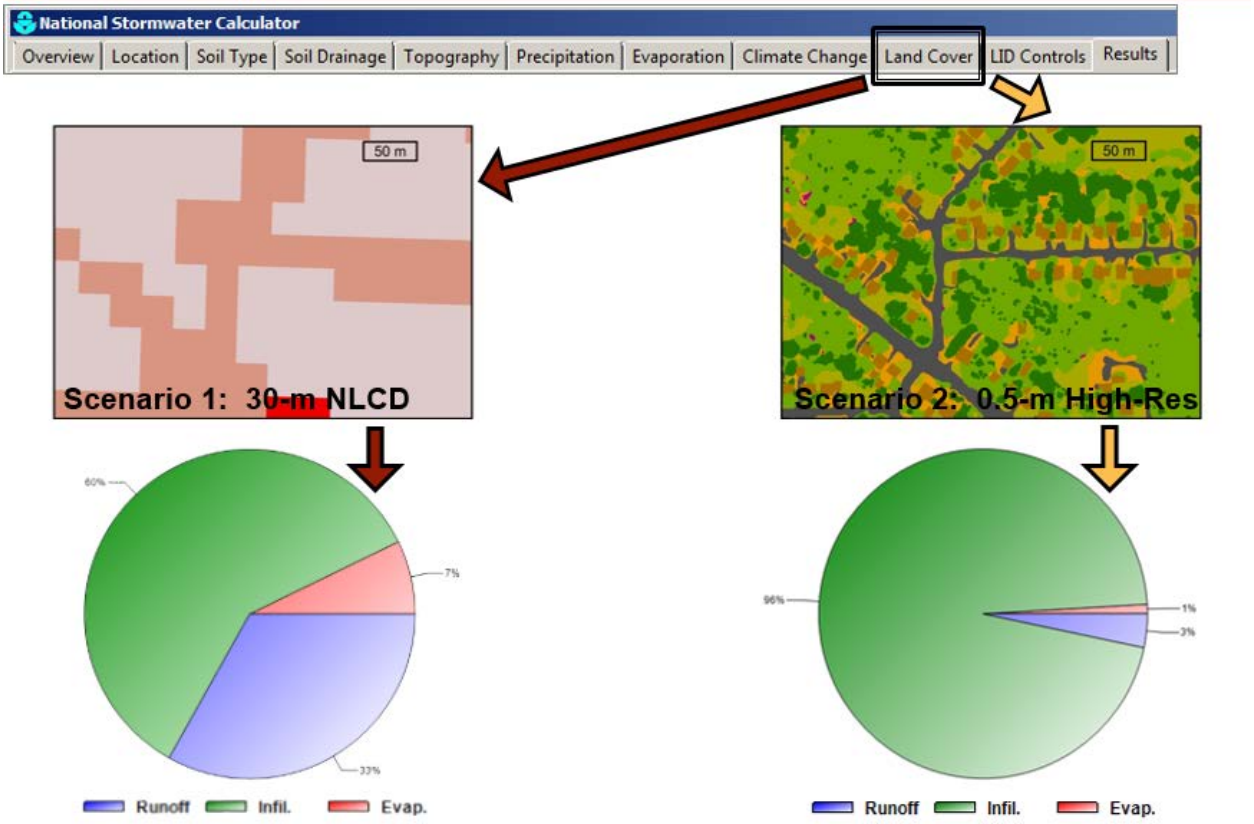

Figure 2. Differences in predicted runoff and infiltration based on NLCD or high resolution land classification using the EPA National Stormwater Model.

For this reason, we initiated this project to expand the Stueve et al. (2014) methodology, which focused on a single watershed, to multiple urban watersheds entering the St. Louis River Estuary (SLRE). We then used these data to develop indices of urban land use intensity, focusing on impervious surface, building footprints, building heights and height diversity within municipal parcels. Finally, we assessed the relationship of these urban land use intensity indices to water quality data collected in nine tributary watersheds of the St. Louis River.

Methods

The study area including Minnesota watersheds draining directly into the St. Louis River estuary, an area of approximately 50,000 ac. (Figure 3).

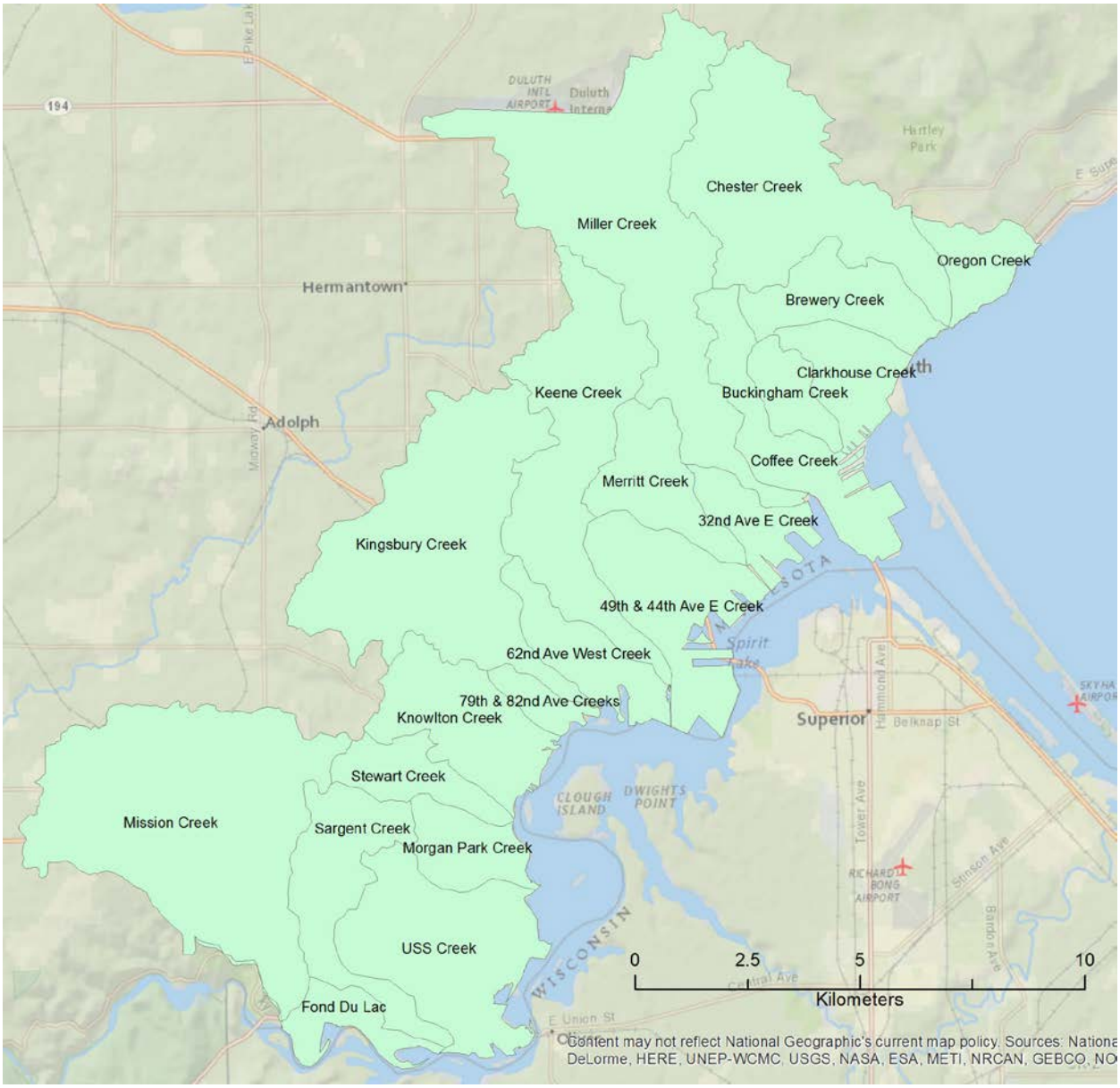

Figure 3. Geographic extent of study, showing watersheds used in Bartsch et al. 2015.

Land use/Land Cover Classification and Analysis

The full detailed methods for the high resolution land classification have been published in Stueve et al. (2014). For much of the spatial extent, we used high resolution (8 cm) color infrared air photos collected by the City of Duluth as part of the 2013 LiDAR collection. To facilitate processing, images were resampled to 0.3 m. For the classification we used the color and NIR bands, as well as the Normalized Difference Vegetation Index (NDVI). For areas outside the City of Duluth footprint, we used 1 m summer 2010 imagery provided by the MN DNR.

There was a LiDAR acquisition for the Arrowhead region of Minnesota in spring 2011. In summer 2012 Duluth experienced a 10” rainfall event that caused severe flooding and over $100,000,000 in damages to buildings and infrastructure. To document flood damage, the State conducted a second LiDAR collection in fall 2012. LiDAR data were used to develop a surface model (DEM) as well as a canopy height model (CHM), both of which were used in the classification. We also used the building footprints and calculated the maximum height of each building. Building heights and the standard deviation of height, an index of complexity, were then summarized by tax parcels provided by the City of Duluth and St. Louis County. LiDAR was also used to classify pavement (roads, sidewalks, parking lots) as impervious surface.

The classification was performed using object-based image analysis (OBIA), using the Feature Analyst extension in ArcGIS 10.1 (Opitz and Blundell 2008). The advantage of OBIA is that it considers the shapes and textures of neighboring pixels in the classification process, which is useful in the patchy landscapes of urban environments. For each landcover type, good, known, representative polygons were used to "train" the software to find similar sets of pixels that represent similar landcover polygons. The software uses "smart", proprietary algorithms to analyze imagery. After an initial attempt to classify and extract is complete, the software was retrained to refine what it correctly, or incorrectly extracted. This process was iterated until satisfactory results were obtained. The classification was repeated for other landcover types, and the resulting rasters (or polygons) merged and mosaicked to develop a complete coverage.

We mapped the following land use/land cover (LULC) classes:

- Deciduous canopy
- Coniferous canopy
- Grass/low shrub canopy
- Impervious surface (roads, building rooftops, parking lots)
- Buildings
- Water

Classification accuracy was assessed by selecting 30 random points per LULC class and comparing them with aerial photographs.

Parcel data were used as a fundamental unit to summarize various aspects of urban land use intensity. For each parcel, we calculated % impervious pavement, % impervious rooftops, and the maximum and standard deviation of building heights. These four variables were scaled 0-1 based on the minimum and maximum values across the full data set, and summed. The summed values were then rescaled 0-1 to create an index of Urban Land Use Intensity (ULUI). We also used the parcel layer to calculate a “greenness” index for each parcel. This index was based on the type of business

associated with the parcel (industrial, commercial, residential), the building/greenspace ratio, and % impervious surface for each parcel.

Using the classified image, we calculated several metrics of landscape complexity - mean patch size, large patch index, and fractal dimension - using the Fragstats spatial analysis program (McGarigal et al. 2012).

Water Quality Analysis

As part of a Sea Grant-funded study of human impacts to watersheds of the St. Louis River estuary (Silbernagel et al. 2015), we collected a suite of water quality data across a gradient of highly urbanized to relatively undisturbed watersheds. The gradient was based on a set of environmental stressors, including road density, population, point source density, as well as urban and agricultural land use (Host et al. 2011). The latter two variables were based on the National Land Cover Dataset (NLCD) classification, with no quantification of the intensity of urban or agricultural land use.

In the larger study, water quality sampling was conducted at 26 sites in the estuary in both nearshore areas and above the mouths of the associated tributaries during multiple flow regimes in 2010-2011 (Bartsch et al 2015). In addition to spring runoff and summer baseflow, we collected water samples at 16 storm events exceeding 0.5 in rainfall. Measured variables included a core suite (temperature (T), dissolved oxygen (DO), specific electrical conductivity (EC25), pH, turbidity, and clarity) of field measurements using a HydroLab multi-parameter sonde (model MS5) and a 120 cm transparency tube. We also analyzed an advanced suite of water quality data, including color, TP, TN, ammonium-N (NH4+-N), nitrite/nitrate-N (NO2-/NO3-N), chloride, sulfate (SO42-), chlorophyll-a (Chl-A), and phaeophytin).

Nine of these watersheds occurred within the geographic extent of the present study. We extracted and resummarized the tributary data from these watersheds for a select set of variables that were highly correlated with the NLCD-based stressor gradient (*SumRel*). These included Chl-A, DO, pH, and chloride. Means of these water quality variable under baseflow and spring runoff conditions were compared with ULUI and greenness scores. These indices were summarized at three spatial scales – across the entire watershed, within a 250 m buffer around the sampling point and within a 100 m buffer.

Results

The classification and derived data layers listed in Table 1 were placed into a geodatabase, downloadable here:
http://data.nrri.umn.edu/data/dataset/duluth-urban-landuse-intensity.
To display the symbology behind the various data sets, we have also include Layer (*.lyr) files.

Table 1. Catalog of Data Layers Developed to Describe Urban Land Use Intensity (geodatabase name: Duluth_Urban_Intensity.gdb)

Layer	Geodatabase Layer Name	Data Type	Resolution	Uncompressed Size	Pixel Depth
LiDAR canopy height model	canopy_height	Raster	1 m	697 MB	8 bit
LiDAR surface model (DEM)	DEM	Raster	1 m	3.35 GB	8 bit
High resolution land classification	Land_cover	Raster	0.5 m	2.25 GB	32 bit
Maximum building height by parcel	parc_height_max	Raster	1 m	576 MB	8 bit
Standard deviation of building height by parcel	parc_height_stddev	Raster	1 m	2.25 GB	32 bit
Greenness score by parcel	parcel_greenness	Raster	3 m	65 MB	8 bit
Impervious surface pavement (percent of parcel)	perc_imp_pave	Raster	1 m	576 MB	8 bit
Impervious surface roof (percent of parcel)	perc_imp_roof	Raster	1 m	576 MB	8 bit
Urban land use intensity index (0.0 - 1.0)	ULUI_index	Raster	1 m	2.25 GB	32 bit
Building footprints - max height	bldg_height	Vector	footprint	NA (30,411 polygons)	NA

Twenty-one watersheds occurred within the study area (Figure 3), ranging in area from 413 to almost 7,000 ac. Deciduous trees were the dominant land cover, averaging 45% across watersheds (Table 2). Impervious pavement averaged 17%, with rooftops adding another 5%. The Urban Land Use Intensity index (ULUI) shows strong fine-scale variation across watersheds (Figure 4), as does the map of greenspace (Figure 5).

Overall classification accuracy was 88%. The two urban classes, impervious surface and buildings, had accuracies of 90% (Table 3). The largest errors were due to difficulties in distinguishing between deciduous and coniferous land cover, neither of which contribute to the ULUI. One aspect of OBIA analyses, however, is that in detecting patterns, the technique will produce polygons that have irregular shapes for objects that are rectilinear in the real world, such as roads or rooftops shaded by trees. This introduces some inaccuracies at the meter scale, but the summaries by parcel presented below average out many of these fine-scale errors.

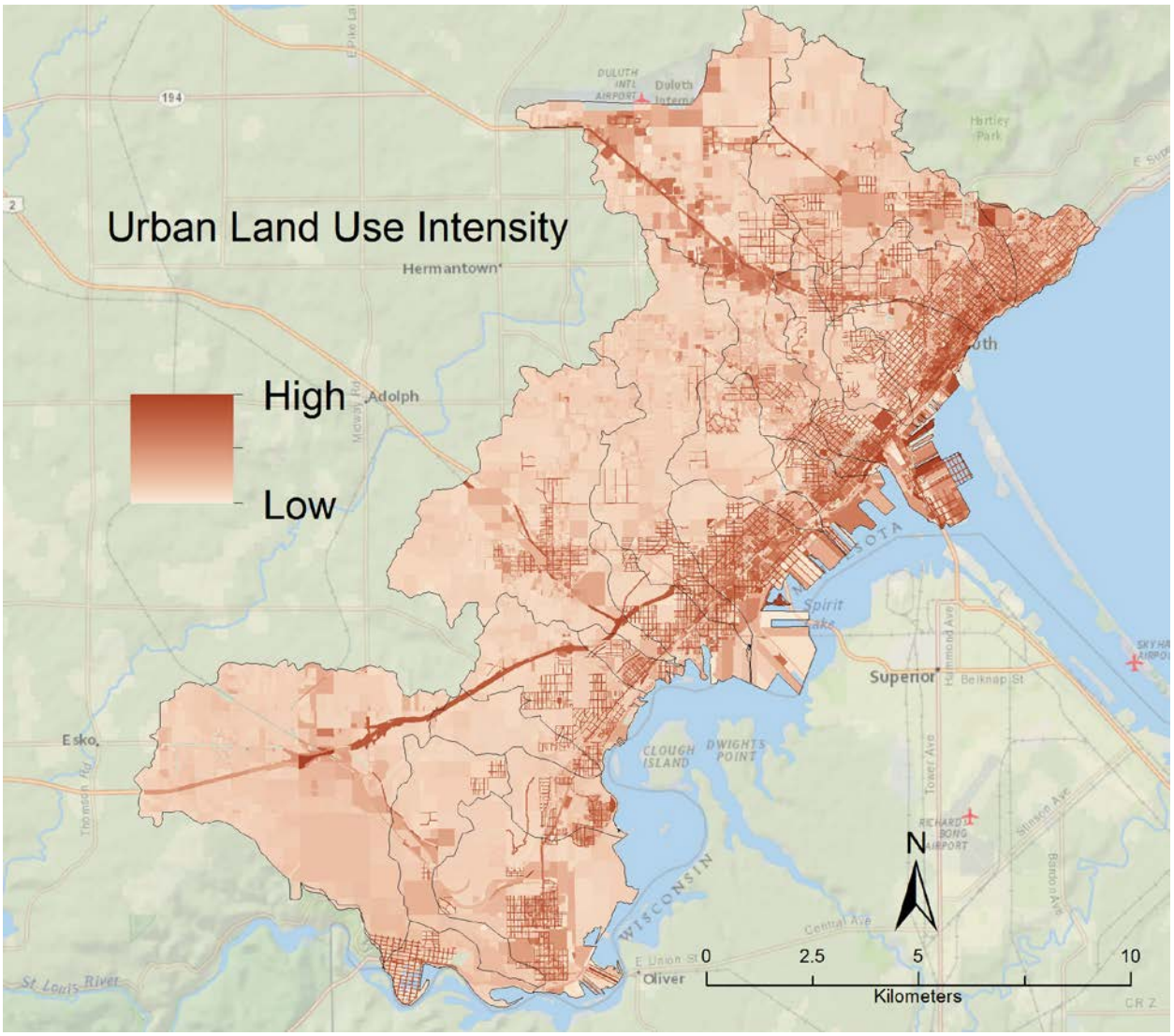

Figure 4. Urban land use intensity index derived from land classification and building information; linework shows watershed boundaries.

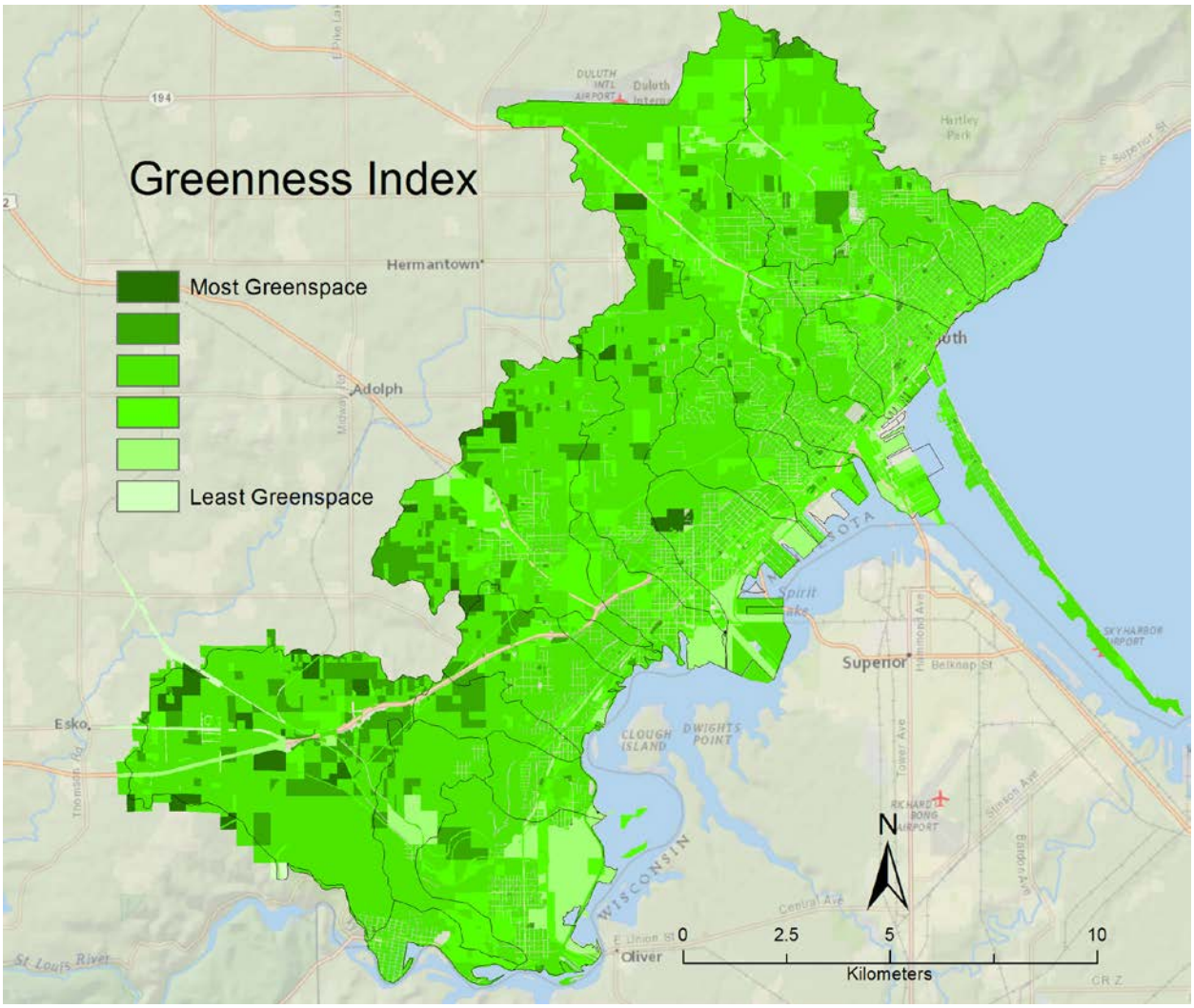

Figure 5. Map of greenness index by parcel, based on the amount of natural vegetation cover, type of business, and amount of impervious surface.

Table 2. Percent of Land Cover and mean urban land use intensity and greenness indices within watersheds.

Watershed	Area (ha)	Area (ac)	Mean ULUI	Mean Greenness Index	% Impervious	% Deciduous	% Conifer	% Building rooftop surfaces	% Grass	% Water	% Undeter-mined
Miller Creek	2499	6174	0.264	2.650	20.79	40.13	15.67	5.05	17.77	0.24	0.35
Oregon Creek	339	838	0.433	2.762	35.88	17.35	21.72	13.89	11.15	0.00	0.00
Keene Creek	1525	3767	0.212	2.978	8.81	55.34	18.86	2.44	14.34	0.18	0.03
Kingsbury Creek	2225	5497	0.200	3.004	7.05	54.54	19.67	2.93	15.44	0.28	0.11
Merritt Creek	580	1434	0.222	2.896	10.62	60.94	11.13	3.39	13.88	0.00	0.04
Stewart Creek	388	958	0.206	3.182	4.09	72.85	16.26	0.76	5.93	0.03	0.09
Sargent Creek	806	1992	0.216	2.743	3.24	72.99	17.62	0.29	5.85	0.00	0.01
Morgan Park Creek	396	979	0.270	2.777	9.82	46.64	33.18	2.54	7.73	0.00	0.08
49th & 44th Ave E Creek	945	2335	0.337	2.492	30.59	29.14	16.36	8.05	12.95	2.08	0.83
32nd Ave E Creek	339	838	0.393	2.389	33.30	34.30	8.35	9.49	14.06	0.25	0.24
Fond Du Lac	315	777	0.279	2.718	6.97	44.89	35.08	0.45	9.48	3.06	0.06
Mission Creek	2820	6969	0.215	3.148	6.45	68.56	12.21	0.51	12.19	0.03	0.06
Knowlton Creek	827	2045	0.253	2.959	7.59	49.46	27.76	1.12	13.48	0.52	0.07
USS Creek	1291	3190	0.253	2.282	9.05	48.63	21.09	2.02	18.26	0.10	0.86
79th & 82nd Ave Creeks	167	413	0.340	2.787	16.42	35.38	26.35	4.25	17.03	0.01	0.58
62nd Ave West Creek	491	1213	0.300	2.271	20.01	25.93	30.33	4.17	18.71	0.29	0.56
Coffee Creek	765	1889	0.397	2.324	31.87	34.99	7.64	7.09	16.90	0.25	1.25
Buckingham Creek	285	704	0.268	2.786	8.77	53.28	9.07	1.69	26.29	0.89	0.01
Clarkhouse Creek	461	1139	0.438	2.509	35.53	29.08	10.01	12.47	12.79	0.10	0.03
Brewery Creek	587	1450	0.390	2.765	29.34	25.58	18.66	11.46	14.91	0.05	0.00
Chester Creek	1819	4494	0.258	2.772	12.37	47.49	19.29	4.29	16.27	0.23	0.06

Table 3. Confusion matrix for classified imagery, based on 30 random points per class.

	Land Cover Classes	Photointerpreted class						Row Totals	Producer's Accuracy (%)
		Building	Water	Grass	Conifer	Deciduous	Impervious		
Classified as:	Building	27	0	1	0	0	2	30	90
	Water	0	30	0	0	0	0	30	100
	Grass	1	0	25	0	4	0	30	83
	Conifer	0	0	0	23	6	1	30	77
	Deciduous	0	0	2	1	27	0	30	90
	Impervious	2	0	1	0	0	27	30	90
Column Totals		30	30	29	24	37	30	180	
User's Accuracy (%)		90	100	86	96	73	90		88 % Overall Accuracy

Basic landscape metrics were calculated at the class and patch scales. Within any class, patch sizes were highly variable. Deciduous trees had large average patch sizes due to expansive areas of forestland outside the urban area. Because of the strong near-continuous connectivity of roads, parking lots, and other paved surfaces, the impervious class also had large patch sizes, as well as the greatest LPI (Table 4). Fractal dimension, a measure of shape complexity, was lowest for water and buildings and highest for forest lands. The high resolution of the classification coupled with the large extent of the study area precluded meaningful calculations of metrics such as lacunarity and Moran's I.

Table 4. Landscape metrics for land use/land cover classes

Land Use/ Land Cover	Class Area (ha)	Mean Patch Size (ha)	Largest Patch Index	Fractal Dimension
Deciduous	9600.48	13.18	0.10	1.43
Conifer	3485.58	0.42	0.02	1.42
Grass/Shrub	2869.97	0.33	0.04	1.34
Impervious	2683.64	9.28	0.21	1.38
Building	754.03	0.07	0.03	1.34
Water	59.10	0.04	0.11	1.31
Undetermined	44.40	0.02	0.03	1.28

Relationships with Water Quality

In spite of the low sample size with respect to watersheds, there were significant relationships between the indices of land use intensity and water quality variables. The previously-published *SumRel* index (Bartsch et al. 2015) was correlated with chlorophyll-A under both spring runoff and baseflow conditions (Table 5). Dissolved oxygen showed strong relationships with ULUI at the watershed scale as well as the greenness index at all three spatial scales. Chloride under baseflow conditions was correlated with ULUI at the 100 and 250 m scales. In general, the more resolved indices of urban land use performed better than *SumRel*, whose land use components were based on NLCD data.

Table 5. Pearson correlations of water quality variables with indices of environmental stress at three spatial scales. Values > 0.4 highlighted in bold.

Water Quality measure	SumRel	Urban Land Use Index			Greenness Index		
	Watershed	250 m buffer	100 m buffer	Watershed	250 m buffer	100 m buffer	Watershed
Chl-A Baseflow	**-0.51**	0.19	-0.02	-0.35	0.18	0.23	0.15
Chl-A Spring	**-0.59**	-0.29	-0.28	-0.02	-0.06	0.01	-0.17
DO-Spring	0.23	0.02	-0.26	**-0.84**	**-0.55**	**-0.53**	**0.60**
pH-Baseflow	**0.51**	0.30	0.26	0.05	-0.13	-0.31	**0.45**
pH-Spring	0.04	**-0.58**	-0.38	0.27	-0.04	-0.19	0.11
Chloride Baseflow	0.19	**0.68**	**0.56**	-0.08	-0.08	0.09	-0.05
Chloride-Spring	-0.18	0.18	0.06	-0.18	0.25	**0.45**	-0.28

Summary

This project conducted a high resolution (3 m) classification of urban land use using categories relevant to managing stream water quality. We used object-oriented image analysis techniques to take advantage of the characteristic spatial patterns of urban areas – square blocks, linear transportation features, and riparian corridors. The spatial data and metadata were uploaded as a geodatabase to this location: *http://data.nrri.umn.edu/data/dataset/duluth-urban-landuse-intensity*

LiDAR data were also used to summarize information on buildings using cadastral data for the City of Duluth and surrounding area. This provides further information on the intensity of land use, under the assumption that the tall buildings of highly urbanized

areas and the diversity of building heights are both related to increased runoff and inputs of urban pollutants into stormwater and stream systems. Building height data were incorporated into an index of urban land use intensity. Comparing these newly-derived indices to previously collected water quality data shows an improvement over models based on coarser-scale land use data (NLCD @ 30 m). The data and analyses presented here provide one more tool to land managers and researchers interesting in quantifying the relationships between environmental stresses from highly modified urban landscapes and the health of aquatic ecosystems.

Acknowledgements

Mr. William Bartsch generously shared the water quality data on St. Louis River estuary tributaries from his Master's thesis. His work was funded through the Joint program of Minnesota and Wisconsin Sea Grants. Dr. Kirk Stueve provided valuable advice on conducting object-based image analyses. This work was funded by the National Oceanic and Atmospheric Administration's Office for Coastal Management.

Literature Cited

Bartsch, W.M., R. P. Axler and G. E. Host. 2015. Evaluating a Great Lakes scale landscape stressor index to assess water quality in the St. Louis River Area of Concern. J. of Great Lakes Research 41:99-110.

Hollenhorst, T. P., T. N. Brown, L. B. Johnson, J. J. H. Ciborowski and G. E. Host. 2007. Methods for generating multi-scale watershed delineations for indicator development in Great Lake coastal ecosystems. Journal of Great Lakes Research 33: 13-26.

Host, G. E., T.N. Brown, T.P. Hollenhorst, L. B. Johnson, and J. J. H. Ciborowski. 2011. High-resolution assessment and visualization of environmental stressors in the Lake Superior basin. Aquatic Ecosystem Health and Management 14: 376-385.

Johnson, L.B. and G.E. Host. 2010. Recent developments in landscape approaches for the study of aquatic ecosystems. J. N. Am. Benthol. Soc. 29:41-66.

Ju, W. and N. Lam. 2007. Urban land use classification: applying texture analysis and artificial intelligence. Imaging Notes Magazine, http://www.imagingnotes.com/go/article_free.php?mp_id=112

Lu, Z. 2010. Pattern analysis and intensity evaluation of urban land use in East Peral Rier Delta, China. 2010 2nd IITA Int. Conf on Geoscience and Remote Sensing, 430-433.

McGarigal, K., SA Cushman, and E Ene. 2012. FRAGSTATS v4: Spatial Pattern Analysis Program for Categorical and Continuous Maps. Computer software program produced by the authors at the University of Massachusetts, Amherst. Available at the following web

site: http://www.umass.edu/landeco/research/fragstats/fragstats.html

Opitz, D. and S. Blundell. 2008. Object recognition and image segmentation: the feature analyst approach. In: Blaschke, T. S. Lang and G. Hay (eds) Object-based image analysis. Springer, Berlin pp 153-167

Silbernagel, J., Host, G., Fortner, R., Axler, R., Danz, N., Smith, V, Mathews, J., Hart, D.,Hagley, C., Wagler, M., Axler, M., Bartsch, W., & A. Drewes. 2015. Linking place-based science to people through spatial narratives of coastal stewardship. J. of Coastal Conservation 19:181-198.

Singh, K. J. B. Vogler and R. K. Meentenmeyer. Estimation of land-use in an urbanized landscape using LIDAR intensity data: a regional scale approach. ASPRS/CaGIS 2010 Fall Conference. Nov 2010 Orlando, FL.

Stueve, K.M., T. P. Hollenhorst, J. R. Kelly, L. B. Johnson and G. E. Host. 2014. High resolution maps of forest-urban watersheds present an opportunity for ecologists and managers. Landscape Ecology 30:313-323.